CFD Transonic Store Separation Trajectory Predictions with Comparison to Wind Tunnel Investigations

Elias E. Panagiotopoulos hpanagio@mech.upatras.gr
Hellenic Military Academy
Vari, Attiki, 16673, Greece

Spyridon D. Kyparissis kyparis@mech.upatras.gr
Mechanical Engineering and
Aeronautics Department
University of Patras
Patras, Rio, 26500, Greece

Abstract

The prediction of the separation movements of the external store weapons carried out on military aircraft wings under transonic Mach number and various angles of attack is an important task in the aerodynamic design area in order to define the safe operational-release envelopes. The development of computational fluid dynamics techniques has successfully contributed to the prediction of the flowfield through the aircraft/weapon separation problems. The numerical solution of the discretized three-dimensional, inviscid and compressible Navier-Stokes equations over a dynamic unstructured tetrahedral mesh approach is accomplished with a commercial CFD finite-volume code. A combination of spring-based smoothing and local remeshing are employed with an implicit, second-order upwind accurate Euler solver. A six degree-of-freedom routine using a fourth-order multi-point time integration scheme is coupled with the flow solver to update the store trajectory information. This analysis is applied for surface pressure distributions and various trajectory parameters during the entire store-separation event at various angles of attack. The efficiency of the applied computational analysis gives satisfactory results compared, when possible, against the published data of verified experiments.

Keywords: CFD Modelling, Ejector Forces and Moments, Moving-body Trajectories, Rigid-body Dynamics, Transonic Store Separation Events.

1. INTRODUCTION

With the advent and rapid development of high performance computing and numerical algorithms, computational fluid dynamics (CFD) has emerged as an essential tool for engineering and scientific analyses and design. Along with the growth of computational resources, the complexity of problems that need to be modeled has also increased. The simulation of aerodynamically driven, moving-body problems, such as store separation, maneuvering aircraft, and flapping-wing flight are important goals for CFD practitioners [1].

The aerodynamic behavior of munitions or other objects as they are released from aircraft is critical both to the accurate arrival of the munitions and the safety of the releasing aircraft [2]. In

the distant past separation testing was accomplished solely using flying tests. This approach was very time-consuming, often requiring years to certify a projectile. It was also expensive and occasionally led to the loss of an aircraft due to unexpected behavior of the store being tested.

In the past, separation testing was accomplished solely via flight tests. In addition to being very time consuming, often taking years to certify a weapon, this approach was very expensive and often led to loss of aircraft. In the 1960s, experimental methods of predicting store separation in wind tunnel tests were developed. These tests have proven so valuable that they are now the primary design tool used. However, wind tunnel tests are still expensive, have long lead times, and suffer from limited accuracy in certain situations, such as when investigating stores released within weapons bays or the ripple release of multiple moving objects. In addition, because very small-scale models must often be used, scaling problems can reduce accuracy.

In recent years, modelling and simulation have been used to reduce certification cost and increase the margin of safety of flight tests for developmental weapons programs. Computational fluid dynamics (CFD) approaches to simulating separation events began with steady-state solutions combined with semi-empirical approaches [3] - [7]. CFD truly became an invaluable asset with the introduction of Chimera overset grid approaches [8]. Using these methods, unsteady full field simulations can be performed with or without viscous effects.

The challenge with using CFD is to provide accurate data in a timely manner. Computational cost is often high because fine grids and small time steps may be required for accuracy and stability of some codes. Often, the most costly aspect of CFD, both in terms of time and money, is grid generation and assembly. This is especially true for complex store geometries and in the case of stores released from weapons bays. These bays often contain intricate geometric features that affect the flow field.

Aerodynamic and physical parameters affect store separation problems. Aerodynamic parameters are the store shape and stability, the velocity, attitude, load factor, configuration of the aircraft and flow field surrounding the store. Physical parameters include store geometric characteristics, center of gravity position, ejector locations and impulses and bomb rack. The above parameters are highly coupled and react with each other in a most complicated manner [9] - 11]. An accurate prediction of the trajectory of store objects involves an accurate prediction of the flow field around them, the resulting forces and moments, and an accurate integration of the equations of motion. This necessitates a coupling of the CFD solver with a six degree of freedom (6-DOF) rigid body dynamics simulator [12]. The simulation errors in the CFD solver and in the 6-DOF simulator have an accumulative effect since any error in the calculated aerodynamic forces can predict a wrong orientation and trajectory of the body and vice-versa. The forces and moments on a store at carriage and various points in the flow field of the aircraft can be computed using CFD applied to the aircraft and store geometry [13].

The purpose of this paper is to demonstrate the accuracy and technique of using an unstructured dynamic mesh approach to store separation. The most significant advantage of utilizing unstructured meshes [14] is the flexibility to handle complex geometries. Grid generation time is greatly reduced because the user's input is limited to mainly generation of a surface mesh. Though not utilized in this study, unstructured meshes additionally lend themselves very well to solution-adaptive mesh refinement/coarsening techniques, especially useful in capturing shocks. Finally, because there are no overlapping grid regions, fewer grid points are required.

The computational validation of the coupled 6-DOF and overset grid system is carried out using a simulation of a safe store separation event from underneath a delta wing under transonic conditions (Mach number 1.2) at an altitude of 11,600 m [15] and various angles of attack (0°, 3° and 5°) for a particular weapon configuration with appropriate ejection forces. An inviscid flow is assumed to simplify the above simulations. The predicted computed trajectories are compared with a 1/20 scale wind-tunnel experimental data conducted at he Arnold Engineering Development Center (AEDC) [16] - [17].

2. WEAPON / EJECTOR MODELLING

In the present work store-separation numerically simulation events were demonstrated on a generic pylon/store geometric configuration attached to a clipped delta wing, as shown in FIGURE 1. Benchmark wind-tunnel experiments for these cases were conducted at the Arnold Engineering Development Center (AEDC) [16], and the details of the data can be found in Lijewski and Suhs [18]. Results available from these studies include trajectory informations and surface pressure distributions at multiple instants in time. The computational geometry matches the experimental model with the exception of the physical model being 1/20 scale.

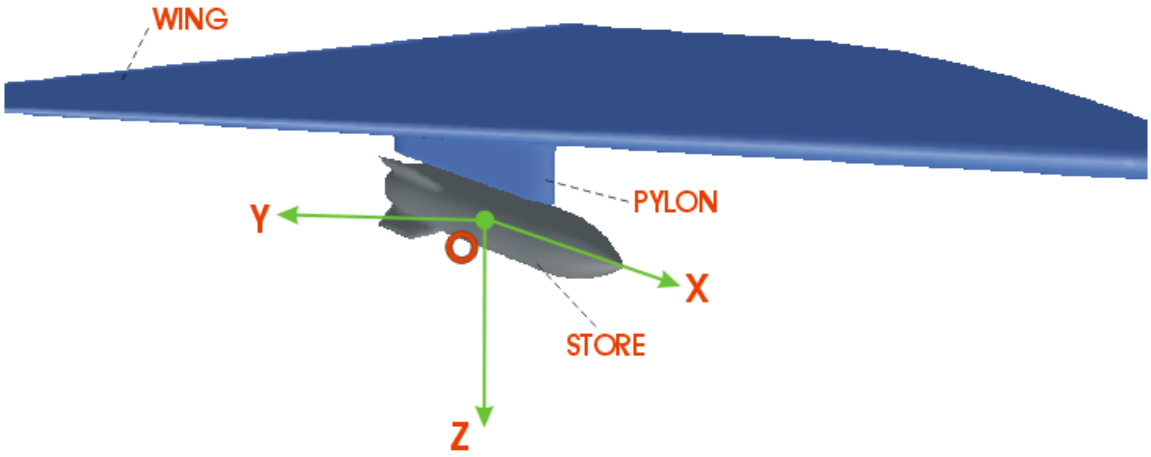

FIGURE 1: Global coordinate system OXYZ for store separation trajectory analysis.

It can be seen from FIGURE 1 the global coordinate system orientation OXYZ for the store separation simulation analysis. The origin O is located at the store center of gravity while in storage. X-axis runs from the tail to nose of the store, Y-axis points away from the aircraft and Z-axis points downward along the direction of the gravity.

The aircraft's wing is a 45-degree clipped delta with 7.62 m (full scale) root chord length, 6.6 m semi-span, and NACA 64A010 airfoil section. The ogive-flat plate-ogive pylon is located spanwise 3.3 m from the root, and extends 61 cm below the wing leading edge. The store consists of a tangent-ogive forebody, clipped tangent-ogive afterbody, and cylindrical centerbody almost 50 cm in diameter. Overall, the store length is approximately 3.0 m. Four fins are attached, each consisting of a 45-degree sweep clipped delta wing with NACA 008 airfoil section. To accurately model the experimental setup, a small gap of 3.66 cm exists between the missile body and the pylon while in carriage.

In the present analysis the projectile is forced away from its wing pylon by means of identical piston ejectors located in the lateral plane of the store, -18 cm forward of the center of gravity (C.G.), and 33 cm aft. While the focus of the current work is not to develop an ejector model for the examined projectile configuration, simulating the store separation problem with an ejector model which has known inaccuracies serves little purpose [9].

The ejector forces were present and operate for the duration of 0.054 s after releasing the store. The ejectors extend during operation for 10 cm, and the force of each ejector is a constant function of this stroke extension with values 10.7 kN and 42.7 kN, respectively. The basic geometric properties of the store and ejector forces for this benchmark simulation problem are tabulated in TABLE 1 and are depicted in a more detail drawing in FIGURE 2.

As the store moves away from the pylon, it begins to pitch and yaw as a result of aerodynamic forces and the stroke length of the individual ejectors responds asymmetrically.

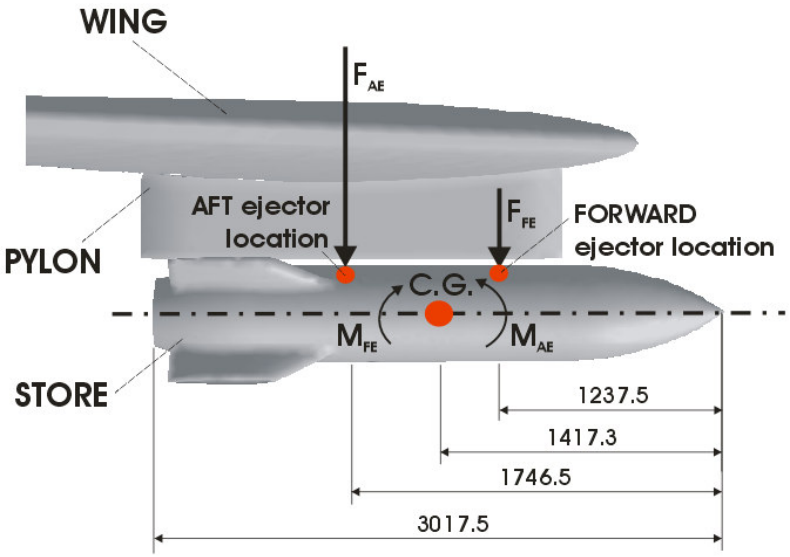

FIGURE 2: Ejector force model for the store separation problem.

Characteristic Magnitudes	Values
Mass m, kg	907
Reference Length L, mm	3017.5
Reference Diameter D, mm	500
No. of fins	4
Center of gravity $x_{C.G.}$, mm	1417 (aft of store nose)
Axial moment of inertia I_{XX}, kg·m^2	27
Transverse moments of inertia I_{yy} and I_{zz}, kg·m^2	488
Forward ejector location $L_{FE.}$, mm	1237.5 (aft of store nose)
Forward ejector force F_{FE}, kN	10.7
Aft ejector location L_{AE}, mm	1746.5 (aft of store nose)
Aft ejector force F_{AE}, kN	42.7
Ejector stroke length L_{ES}, mm	100

TABLE 1: Main geometrical data for the examined store separation projectile.

3. FLOWFIELD NUMERICAL SIMULATION

The computational approach applied in this study consists of three distinct components: a flow solver, a six degree of freedom (6DOF) trajectory calculator and a dynamic mesh algorithm [12]. The flow solver is used to solve the governing fluid-dynamic equations at each time step. From this solution, the aerodynamic forces and moments acting on the store are computed by integrating the pressure over the surface. Knowing the aerodynamic and body forces, the

movement of the store is computed by the 6DOF trajectory code. Finally, the unstructured mesh is modified to account for the store movement via the dynamic mesh algorithm.

3.1 Flow Solver

The flow is compressible and is described by the standard continuity and momentum equations. The energy equation incorporates the coupling between the flow velocity and the static pressure. The flow solver is used to solve the governing fluid dynamic equations that include an implicit algorithm for the solution of the Euler Equations [11] - [14]. The Euler equations are well known and hence, for purposes of brevity, are not shown. The present analysis employs a cell-centered finite volume method based on the linear reconstruction scheme, which allows the use of computational elements with arbitrary polyhedral topology. A point implicit (block Gauss-Seidel) linear equation solver is used in conjunction with an algebraic multigrid (AMG) method to solve the resultant block system of equations for all dependent variables in each cell. Temporally, a first order implicit Euler scheme is employed [14] - [23].

The conservation equation for a general scalar f on an arbitrary control volume whose boundary is moving can be written in integral form as:

$$\frac{\partial}{\partial t}\int_V \rho f dV + \int_{\partial V} \rho f\left(\vec{u}-\vec{u}_g\right)d\vec{A} = \int_{\partial V} I\nabla f d\vec{A} + \int_V S_f dV \tag{1}$$

The time derivative in Eq.(1) is evaluated using a first-order backward difference formula:

$$\frac{d}{dt}\int_V \rho f dV = \frac{\left(\rho f V\right)^{k+1} - \left(\rho f V\right)^{k}}{\Delta t} \tag{2}$$

where the superscript denotes the time level and also

$$V^{k+1} = V^{k} + \frac{dV}{dt}\Delta t \tag{3}$$

The space conservation law [24] is used in formulating the volume time derivative in the above expression Eq.(3) in order to ensure no volume surplus or deficit exists.

3.2 Trajectory Calculation

The 6DOF rigid-body motion of the store is calculated by numerically integrating the Newton-Euler equations of motion within Fluent as a user-defined function (UDF). The aerodynamic forces and moments on the body store are calculated based on the integration of pressure over the surface. This information is provided to the 6DOF from the flow solver in inertial coordinates. The governing equation for the translational motion of the center of gravity is solved for in the inertial coordinate system, as shown below:

$$\dot{\vec{v}}_G = m\sum \vec{f}_G \tag{4}$$

where $\dot{\vec{v}}_G$ is the translational motion of the center of gravity, m is the mass of the store and $\vec{f}_G$ is the force vector due to gravity.

The angular motion of the moving object $\vec{\omega}_{\mathrm{B}}$, on the other hand, is more readily computed in body coordinates to avoid time-variant inertia properties:

$$\dot{\vec{\omega}}_{\mathrm{B}} = L^{-1}\left(\sum \vec{M}_B - \vec{\omega}_{\mathrm{B}} \times L\vec{\omega}_{\mathrm{B}}\right) \tag{5}$$

where L is the inertia tensor and $\vec{M}_B$ is the moment vector of the store.
The orientation of the store is tracked using a standard 3-2-1 Euler rotation sequence. The moments are therefore transformed from inertial to body coordinates via

$$\vec{M}_B = R\vec{M}_G \tag{6}$$

where R is the transformation matrix

$$R \equiv \begin{bmatrix} c_\theta c_\psi & c_\theta s_\psi & -s_\theta \\ s_\phi s_\theta c_\psi - c_\phi s_\psi & s_\phi s_\theta s_\psi + c_\phi c_\psi & c_\theta s_\phi \\ c_\phi s_\theta c_\psi + s_\phi s_\psi & c_\phi s_\theta s_\psi - s_\phi c_\psi & c_\theta c_\phi \end{bmatrix} \tag{7}$$

with the shorthand notation $c_\xi = \cos(\xi)$ and $s_\xi = \sin(\xi)$ has been used.
Once the translational and angular accelerations are computed from Eqs (4) and (5), the angular rates are determined by numerically integrating using a fourth-order multi-point Adams-Moulton formulation:

$$\xi^{k+1} = \xi^k + \frac{\Delta t}{24}\left(9\dot{\xi}^{k+1} + 19\dot{\xi}^k - 5\dot{\xi}^{k-1} + \dot{\xi}^{k-2}\right) \tag{8}$$

where ξ represents either $\vec{v}_G$ or $\vec{\omega}_B$.

The dynamic mesh algorithm takes as input $\vec{v}_G$ and $\vec{\omega}_G$. The angular velocity, then, is transformed back to inertial coordinates via

$$\vec{M}_G = R^T\vec{M}_B \tag{9}$$

where R is given in Eq.(7).

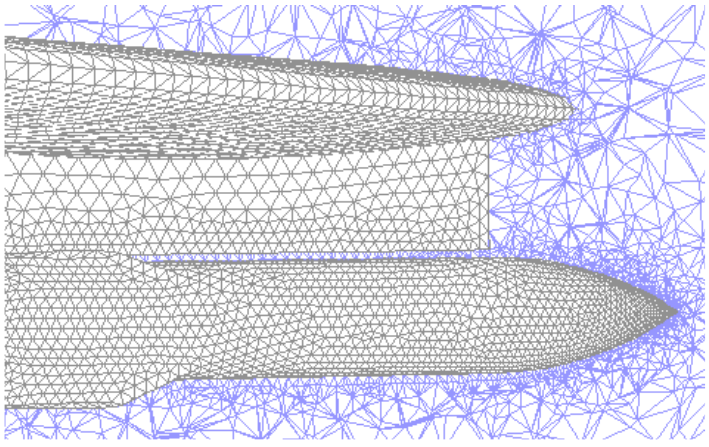

FIGURE 3: Refined mesh in the region near the store.

3.3 Dynamic Mesh

The geometry and the grid were generated with Fluent's pre-processor, Gambit® using tetrahedral volume mesh [25]. As shown in FIGURE 3, the mesh of the fluid domain is refined in the region near the store to better resolves the flow details. In order to simulate the store separation an unstructured dynamic mesh approach is developed. A local remeshing algorithm is

used to accommodate the moving body in the discretized computational domain. The unstructured mesh is modified to account for store movement via the dynamic mesh algorithm.

FIGURE 4: Surface mesh of the examined store.

When the motion of the moving body is large, poor quality cells, based on volume or skewness criteria, are agglomerated and locally remeshed when necessary. On the other hand, when the motion of the body is small, a localized smoothing method is used. That is, nodes are moved to improve cell quality, but the connectivity remains unchanged. A so-called spring-based smoothing method is employed to determine the new nodal locations. In this method, the cell edges are modeled as a set of interconnected springs between nodes.

The movement of a boundary node is propagated into the volume mesh due to the spring force generated by the elongation or contraction of the edges connected to the node. At equilibrium, the sum of the spring forces at each node must be zero; resulting in an iterative equation:

$$\Delta\vec{x}_i^{m+1} = \frac{\sum_{j=1}^{n_i} k_{ij}\Delta\vec{x}_i^{m}}{\sum_{j=1}^{n_i} k_{ij}} \tag{10}$$

where the superscript denotes iteration number. After movement of the boundary nodes, as defined by the 6DOF, Eq.(10) is solved using a Jacobi sweep on the interior nodes, and the nodal locations updated as

$$\vec{x}_i^{k+1} = \vec{x}_i^{k} + \Delta\vec{x}_i \tag{11}$$

where here the superscript indicates the time step.

In FIGURE 4 the surface mesh of the store is illustrated. A pressure far field condition was used at the upstream and downstream domain extents. The initial condition used for the store-separation simulations was a fully converged steady-state solution [26] - [28]. This approach was demonstrated on a generic wing-pylon-store geometry with the basic characteristics shown on the previous section. The domain extends approximately 100 store diameters in all directions around the wing and store.

The working fluid for this analysis is the air with density ρ = 0.33217 kg/m^3. The studied angles of attack are 0°, 3° and 5°, respectively. The store separation is realized to an altitude of 11,600 m, where the corresponding pressure is 20,657 Pa and the gravitational acceleration is g = 9.771 m/s^2. The Mach number is M = 1.2 and the ambient temperature is T = 216.65 K [15], [29], [30].

4. NUMERICAL ANALYSIS RESULTS

The full-scale separation events are simulated under transonic conditions (Mach number 1.2) at an altitude of 11,600 m and various angles of attack (0°, 3° and 5°) using CFD-FLUENT package

[31] - [32]. The initial condition used for the separation analysis was a fully converged steady-state solution. Because an implicit time stepping algorithm is used, the time step Δt is not limited by stability of the flow solver. Rather, Δt is chosen based on accuracy and stability of the dynamic meshing algorithm. Time step Δt = 0.002 sec is chosen for the convergence of store-separation trajectory simulations.

Four trajectory parameters are examined and compared with the experimental data: center of gravity (CG) location, CG velocity, orientation, and angular rate. These parameters are plotted in FIGURE 5 - 8 for total store separation process in 0.8 sec. In each plot are shown the experimental data at α = 0 deg [30], [33], [34] and CFD data for the three examined angles of attack.

FIGURE 5 shows the store CG location in the global coordinate system as a function of store-separation time. It is apparent that the z (vertical) position matches very closely with the experimental data for the three examined angles of attack. This is because the ejector and gravity forces dominate the aerodynamic forces in this direction. In the x and y direction the agreement is also very good. The store moves rearward and slightly inboard as it falls. The small discrepancy in the x direction is expected because the drag is underestimated in the absence of viscous effects. This is also seen in the CG velocities, shown in FIGURE 6. As expected, the store continuously accelerates rearward, with the CFD results underpredicting the movement for the three examined angles of attack. The store is initially pulled slightly inboard, but soon begins to move slowly outboard with the wing outwash. As with position, the velocity in the z direction matches very well with the experiments for zero angle of attack. In this plot the effect of the ejectors is seen clearly at the beginning of the trajectory via a large z-velocity gradient. After approximately t = 0.05 seconds, the store is clear of the ejectors.

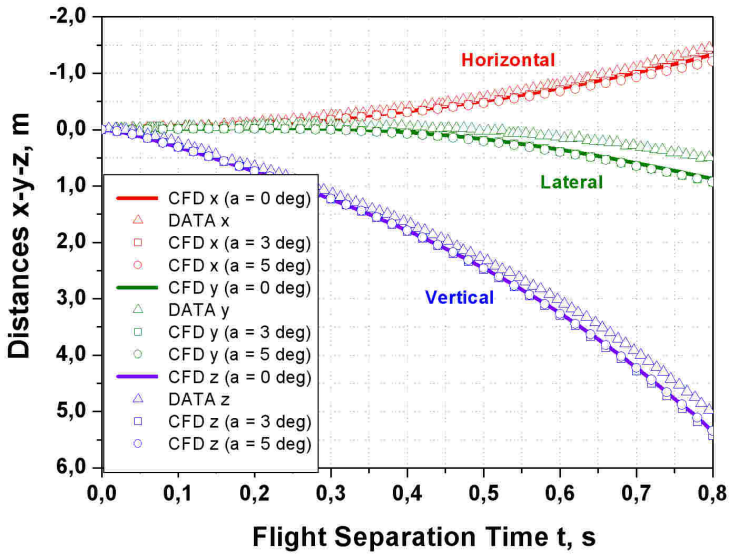

FIGURE 5: Center of gravity location.

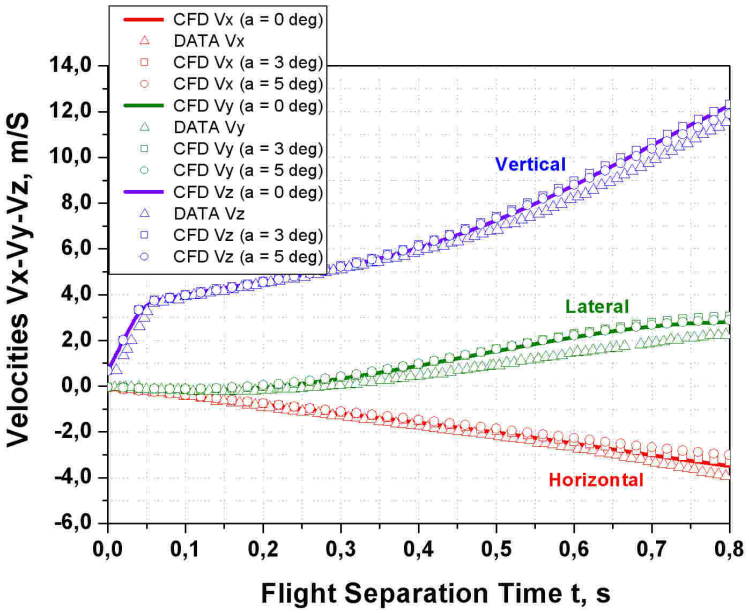

FIGURE 6: Center of gravity velocity.

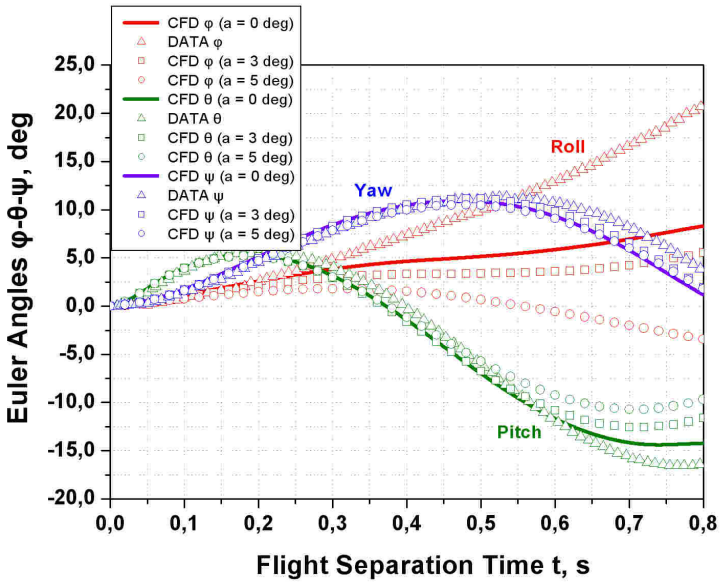

FIGURE 7: Angular orientation of projectile separation process.

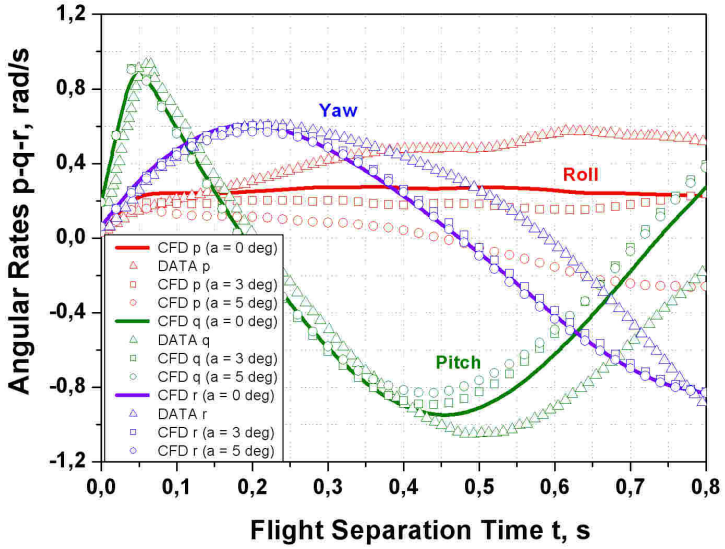

FIGURE 8: Angular rate of the examined store movement.

The orientation of the store is more difficult to model than the CG position. This is evident in FIGURE 7, which shows the Euler angles as a function of time. The pitch and yaw angles agree well with the experiment for α = 0, 3 and 5 degrees, respectively. The store initially pitches nose-up in response to the moment produced by the ejectors, as shown in FIGURE 2. Once free of the ejectors after 0.05 seconds, though, the nose-down aerodynamic pitching moment reverses the trend. The store yaws initially outboard until approximately 0.55 seconds, after which it begins turning inboard. The store rolls continuously outboard throughout the first 0.8 seconds of the separation. This trend is under-predicted by the CFD simulation analysis, and the curve tends to diverge from the experiments after approximately 0.3 seconds for all the examined angles of attack. The roll angle is especially difficult to model because the moment of inertia about the roll axis is much smaller than that of the pitch and yaw axes, see TABLE 1. Consequently, roll is very sensitive to errors in the aerodynamic force prediction. The body angular rates are plotted in FIGURE 8. Here again it is shown that the pitch and yaw rates compare well with the experiments at α = 0 deg, while the roll rate is more difficult to capture.

It is obvious, that the CFD performs very well in modelling the whole store separation events. This is reiterated in FIGURE 9, in which views of the simulated store movements at α = 0 and α = 5 deg, respectively, are compared at discrete instants in time throughout the separation for the first 0.8 seconds. In the examined two cases the stores pitch down even though the applied ejector forces causes a positive (nose up) ejector moment and roll inboard and yaw outboard. This downward pitch of the store is a desirable trait for safe separation of a store from a fighter aircraft [2].

The fluid dynamics prediction analysis also gives pressure coefficient distributions for the total separation history along axial lines on the store body at four circumferential locations and three instants in time. The simulation data are compared with experimental surface pressure data from the wind tunnel tests [31], [33], 34], as depicted in FIGURES 10 up to 13.

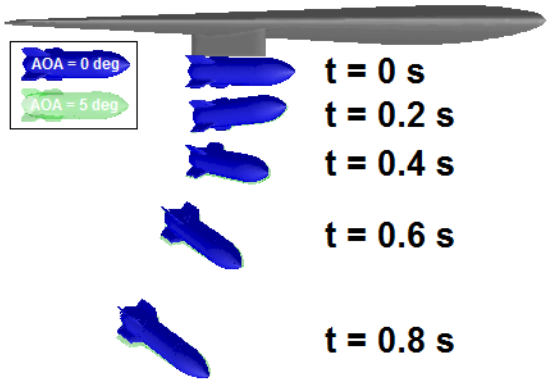

(a) Front view with side angles

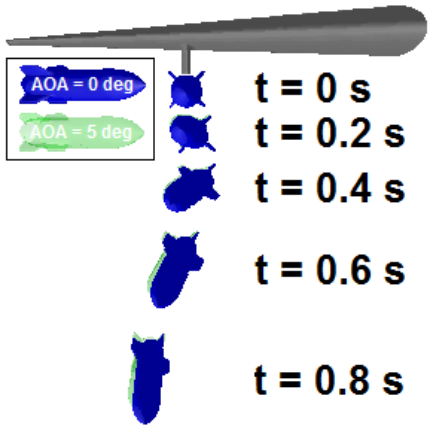

(b) Front view

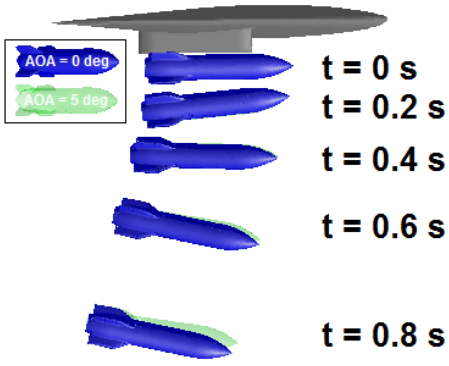

(c) Side view

FIGURE 9: Store separation events with ejectors at Mach 1.2 for 0 and 5 deg angle of attacks, respectively.

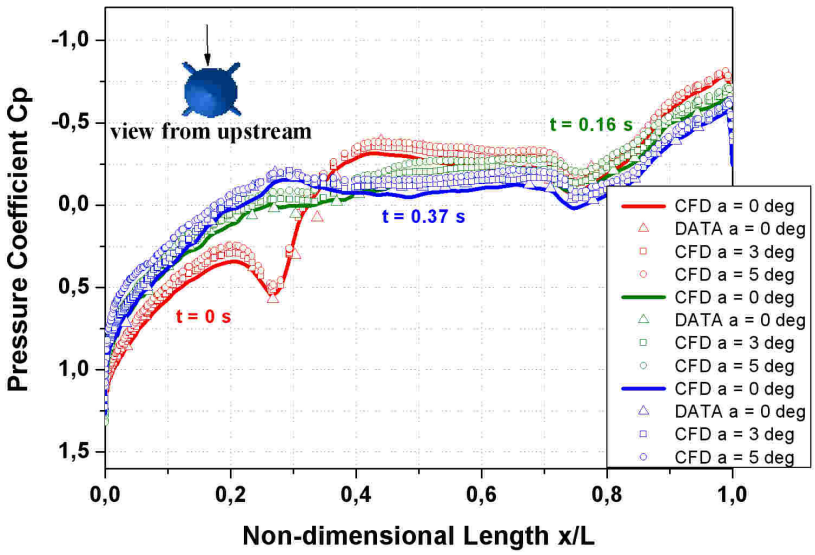

FIGURE 10: Surface pressure profile for phi = 5 deg.

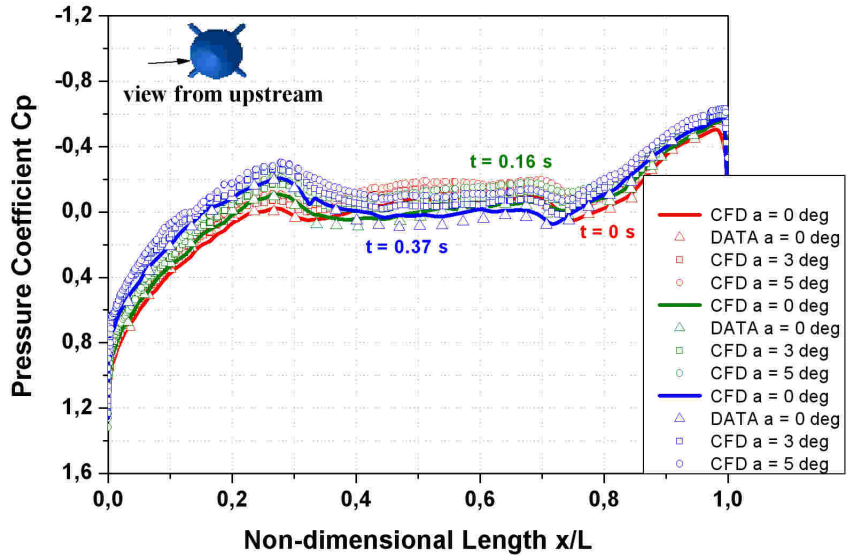

FIGURE 11: Surface pressure profile for phi = 95 deg.

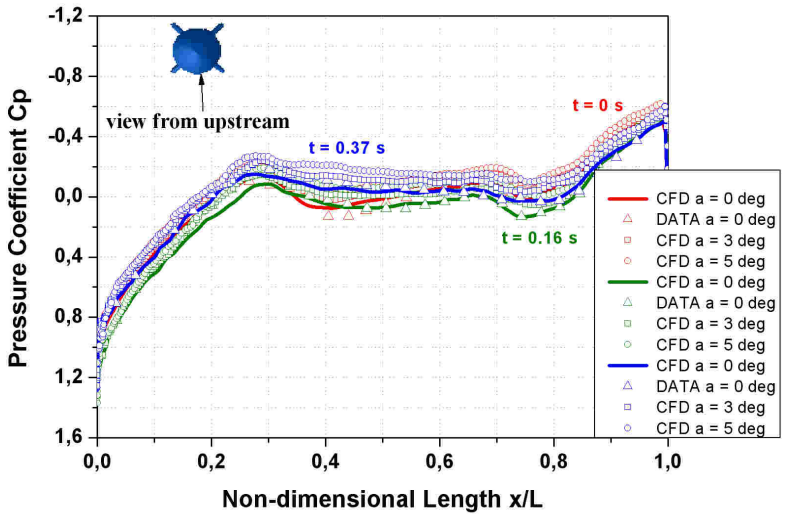

FIGURE 12: Surface pressure profile for phi = 185 deg.

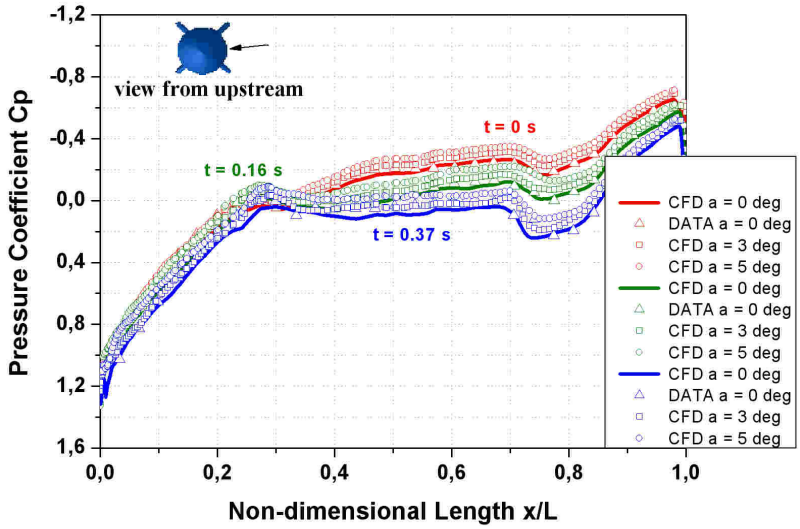

FIGURE 13: Surface pressure profile for phi = 275 deg.

The circumferential locations are denoted by the angle phi. The value phi = 0 is located at the top (y = 0, nearest the pylon) of the store while in carriage and is measured counter clockwise when viewed from upstream. FIGURES 10 - 13 show the pressure profiles along the non-dimensional axis of symmetry length x/L at phi = 5, 95, 185, and 275 deg for three time instants t = 0.0, 0.16, and 0.37 seconds with 0°, 3° and 5° degrees angle of attack (blue, green and red solid lines), respectively. It is obvious the agreement between computational and experimental data, especially in the region near the nose of projectile where the pressure coefficient Cp takes positive values.

The CFD numerical results correspond to the nominal grid with time step Δt = 0.002 sec run. Agreement is exceptional. Of particular interest is the phi = 5 deg line at t = 0.0 because it is

located in the small gap between the pylon and store. The deceleration near the leading edge of the pylon is apparent at x/L = 0.25, and is well captured.

Also FIGURE 14 shows the zero angle of attack Cp computational results at five different times of the store separation process along the axis of symmetry passing from the fin tail. Strong disturbances are noticed in this diagram in the fin tail region x/L = 0.7 to 1.0 where the presence of the fin influences the air flow field environment around the projectile process separation. The computational results show that Cp takes positive values not only at distances close to projectile's nose region but also at the leading edge region of the backward fin tail.

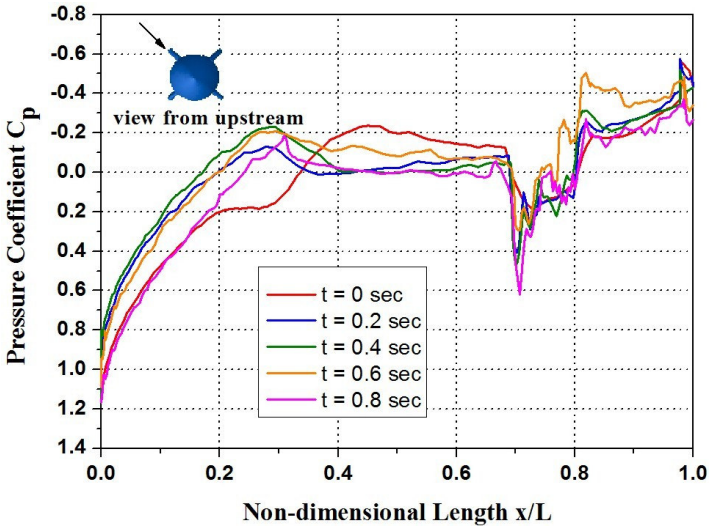

FIGURE 14: Surface pressure profiles along the non-dimensional axis of symmetry passing from the projectile fin tail at zero angle of attack.

The above results showed that CFD performed very well in modelling a separation event at transonic Mach number 1.2 for 11,600 m altitude at the three examined angles of attack. The store moved rearward and slightly inboard as it fell in all cases. Consequently the roll is very sensitive to errors in aerodynamic force prediction. In this case, the store initially pitched nose-up in response to the moment produced by the ejectors. Once free of the ejectors, the nose-down aerodynamic pitching moment reversed the trend. The store yawed initially outboard until about 0.55 s, after which it began turning inboard. The store rolled continuously outboard throughout the first 0.8 s of the separation process.

5. CONSLUSION & FUTURE WORK

The current work demonstrates an integrated package for performing 6-DOF simulations coupled with an Euler code. The feasibility of numerical simulation for store separation has been successfully demonstrated in this work. CFD has gradually become a valuable tool for supporting store separation studies and assessments. CFD is very useful and allows the complex geometries associated with real aircraft to be modelled. The modelling of a full aircraft configuration for the Navier-Stokes solution using structured grids is a challenge.

This study has shown that CFD with unstructured dynamic meshing can be an effective and successful tool for modelling transonic store separation at various angles of attack. The simulation captured the experimental location, velocity, orientation, and angular rate trends. Surface pressure distributions were also in good agreement with experiments at three times during the whole separation event.

This approach offers the ability to obtain accurate store separation predictions with quick turn-around times. Benefits include fast grid generation due to the use of unstructured tetrahedral

meshes, and a fully parallelized, accurate, and stable solver that allows small grids and relatively large time steps. Grid generation can be accomplished in a matter of hours, and runs such as the nominal grid case with time step $\Delta t = 0.002$ seconds examined in this study can be completed overnight on a desktop workstation.

Some error did exist between the simulation and experiment, most prominently in the roll angle. Sources of error include the inviscid assumption (resulting in an under-prediction of drag forces) and the quasi-steady nature of the experiment.

Future work is planned to address the viscous effects. Modeling of the boundary layer requires construction of a rigid viscous mesh attached to the store. Additionally, an adaptive grid refinement algorithm is to be added to the solution procedure, providing more accurate prediction of shock strengths and locations to improve the aerodynamic model.

6. REFERENCES

1. A. Arabshahi, D. L. Whitfield. *"A Multi-Block Approach to Solving the Three-Dimensional Unsteady Euler Equations about a Wing-Pylon-Store Configuration".* AIAA Paper 89-3401, August 1989
2. E. E. Covert. *"Conditions for Safe Separation of External Stores".* Journal of Aircraft, 18(8), 1981
3. W. L. Sickles, C. H. Morgret, A. G. Denny and R. H. Nichols. *"Comparison of Time-Accurate CFD and Engineering Methods for the JDAM Separation from an F-18C Aircraft"*. In proceedings of the Aircraft-Store Compatibility Symposium sponsored by International Test and Evaluation Association, Joint Ordinance Commanders Group, Aircraft Store Compatibility Subgroup, Destin, FL, March 5–8, 2001
4. W. L. Sickles, A. G. Denny and R. H. Nichols. *"Time-Accurate CFD Store Separation Predictions with Comparison to Flight Data"*. AIAA Paper No. 2000-0796, In proceedings of the 37th Aerospace Sciences Meeting and Exhibit, Reno, NV, January 10–13, 2000
5. A. Cenko, E. N. Tinoco, R. D. Dyer and J. DeJongh. *"PANAIR Applications to Weapons Carriage and Separation"*. Journal of Aircraft, 18:128–134, 1981
6. E. Ray. *"CFD Applied to Separation of SLAM-ER from the S-3B".* AIAA Paper No. 2003-4226, In proceedings of the AIAA 21st Applied Aerodynamics Conference, Orlando, Florida, June 23–26, 2003
7. S. M. Murman, M. J. Aftosmis and M. J. Berger. *"Simulations of Store from an F/A-18 with a Cartesian Method".* Journal of Aircraft, 41(4):870–878, 2004
8. N. C. Prewitt, D. M. Belk, Soni and W. Shyy. *"Parallel Computing of Overset Grids for Aerodynamic Problems with Moving Objects".* Progress in Aerospace Sciences, 36(2):117-172, 2000
9. K. S. Keen. *"New Approaches to Computational Aircraft/Store Weapons Integration"*. AIAA Paper No. 90-0274, In proceedings of the AIAA 28th Aerospace Sciences Meeting, Reno, NV, January 8–11, 1990
10. T. L. Donegan, J. H. Fox. *"Analysis of Store Trajectories from Tactical Fighter Aircraft".* AIAA Paper No. 91-0183, In proceedings of the AIAA 29th Aerospace Sciences Meeting, Reno, NV, January 7–10, 1991
11. W. L. Sickles, M. J. Rist, C. H. Morgret, S. L. Keeling, K. N. Parthasarathy. *"Separation of the Pegasus XL from an L-1011 Aircraft".* AIAA Paper No. 94-3454, In proceedings of the AIAA Atmospheric Flight Mechanics Conference, August 1–3, 1994
12. R. Koomullil, G. Cheng, B. Soni, R. Noack and N. Prewitt. *"Moving-body Simulations Using Overset Framework with Rigid Body Dynamics".* Mathematics and Computers in Simulation, 78(5-6):618-626, 2008
13. R. Meyer, A. Cenko and S. Yaros. *"An Influence Function Method for Predicting Aerodyanmic Characteristics During Weapon Separation".* In proceedings of the 12th Navy Symposium on Aeroballistics, May 1981

14. S. E. Kim, S. R. Mathur, J. Y. Murthy and D. Choudhury. *"A Reynolds –Averaged Navier-Stokes Solver Using Unstructured Mesh-Based Finite-Volume Scheme"*. AIAA Paper 98-0231, 1998
15. E. E. Panagiotopoulos and S. D. Kyparissis. *"Computational Flowfield Investigation of Store Separation Trajectories from Transonic Aircraft Wing".* International Review of Aerospace Engineering, 2(3):139-144, 2009
16. R. R. Heim. *"CFD Wing/Pylon/Finnned Store Mutual Interference Wind Tunnel Experiment".* AEDC-TSR-91-P4, 1991
17. L. E. Lijewski. *"Comparison of Transonic Store Separation Trajectory Predictions Using the Pegasus/DXEagle and Beggar Codes".* AIAA Paper 97-2202, 1997
18. L. E. Lijewski, N. E. Suhs. *"Time-Accurate Computational Fluid Dynamics Approach to Transonic Store Separation Trajectory Prediction".* Journal of Aircraft, 31(4):886-891, July 1994
19. L. H. Hall, C. R. Mitchell and V. Parthasarathy. *"An Unsteady Simulation Technique for Missile Guidance and Control Applications".* AIAA Paper AIAA97-0636, 1997
20. S. Westmoreland. *"A Comparison of Inviscid and Viscous Approaches for Store Separations".* AIAA Paper AIAA2002-1413, 2002
21. A. Benmeddour, F. Fortin, T. Amirlatifi and N. Stathopoulos. *"Prediction of the CF-18/MK-83 LD Store Separation Characteristics Using a Quasi-Steady CFD Approach".* AIAA Paper No. 2003-4222, In proceedings of the AIAA 21st Applied Aerodynamics Conference, Orlando, Florida, June 23–26, 2003
22. L. Formaggia, J. Peraire and K. Morgan. *"Simulation of a Store Separation Using the Finite Element Method"*. Journal of Applied Mathematical Modelling, 12(2):175–181, 1988
23. E. Lath, K. Kailasanath and R. Lockner. *"Supersonic Flow over an Axisymmetric Backward-Facing Step"*. Journal of Spacecraft and Rockets, 29(3): 352-359, 1992
24. I. Demirdzic, M. Peric. "*Space Conservation Law in Finite Volume Calculations of Fluid Flow*". International Journal for Numerical Methods in Fluids, 8: 1037-1050, 1988
25. R. W. Tramel, R.H. Nichols. *"A Highly Efficient Numerical Method for Overset-Mesh Moving-Body Problems".* AIAA Paper 97-2040, In proceedings of the AIAA 13th Computational Fluid Dynamics Conference, Snowmass Village, CO, June 29–July 2, 1997
26. R. D. Thomas, J. K. Jordan. *"Investigation of Multiple Body Trajectory Prediction Using Time Accurate Computational Fluid Dynamics"*. AIAA Paper AIAA95-1870, 1995
27. R. M. Lee. *"Beggar Code Implementation of the 6DOF Capability for Stores with Moving Components".* AIAA Paper AIAA2004-1251, 2004
28. J. K. Jordan, N. E. Suhs, R. D. Thoms, R. W. Tramel, J. H. Fox and J. C. Erickson. *"Computational Time-Accurate Body Movement Methodology, Validation, and Application".* AEDC-TR-94-15, October 1995
29. J. H. Fox, T. L. Donegan, J. L. Jacocks and R. H. Nichols. *"Computed Euler Flowfield for a Transonic Aircraft with Stores"*. Journal of Aircraft, 28(6):389–396, 1991
30. L. E. Lijewski. *"Transonic Euler Solutions on Mutually Interfering Finned Bodies".* AIAA Journal, 28(6):982-988, June 1990
31. Gambit Modeling Guide, Fluent Incorporated, Lebanon, NH, 1998
32. TGrid 3.4 User's Guide, Fluent Incorporated, Lebanon, NH, 2001
33. J. B. Carman, D. W. Hill and J. P. Christopher. *"Store Separation Testing Techniques at the Arnold Engineering Development Center, Volume II: Description of Captive Trajectory Store Separation Testing in the Aerodynamic Wind Tunnel (4T)".* AEDC-TR-79-1, Vol. II (AD-A087561), 1980
34. C. H. Morgret, R. E. Dix and L. E. Lijewski. *"Development of Analytical and Experimental Techniques for Determining Store Airload Distribution".* Journal of Spacecraft and Rockets, 19(6):489–495, 1982